Reductant free green synthesis of magnetically recyclable MnFe₂O₄@SiO₂-Ag core-shell nanocatalyst for the direct reduction of organic dye pollutants

Ali Serol ERTÜRK[1] , **Gökhan ELMACI[2,*]** , **Mustafa Ulvi GÜRBÜZ[3]**
[1]Department of Analytical Chemistry, Faculty of Pharmacy, Adıyaman University, Adıyaman, Turkey
[2]Department of Chemistry, School of Technical Sciences, Adıyaman University, Adıyaman, Turkey
[3]Department of Chemistry, Faculty of Arts and Sciences, Yıldız Technical University, İstanbul, Turkey

Abstract: The present paper describes *in situ* green immobilization of silver nanoparticles on MnFe₂O₄@SiO₂ nanospheres using *Epilobium parviflorum* (*EP*) without using any other toxic chemicals and reducing or stabilizing agents. The morphology, composition, and magnetic properties of the resulting MnFe₂O₄@SiO₂-Ag core-shell nanocatalyst were characterized by scanning electron microscope (SEM), transmission electron microscopy (TEM), thermogravimetric analysis (TGA), X-ray diffraction (XRD), vibrating sample magnetometer (VSM), and attenuated total reflectance-Fourier transform infrared spectroscopy (ATR-FTIR). The catalytic performance of the synthesized MnFe₂O₄@SiO₂-Ag was employed on the organic pollutants dyes such as rhodamine B (RhB) and methylene blue (MB). The results revealed significant reduction performances for the MB (116.28 s^{-1} g^{-1}) and RhB (27.12 s^{-1} g^{-1}) over the existing literature. Furthermore, the MnFe₂O₄@SiO₂-Ag exhibited high stability for the completion of the reduction of RhB between the reaction times of 13.1 (first) and 19.8 min (final) with the 100% decolorization efficiency even after several cycles with an excellent magnetic separation. Overall, this work demonstrates a simple and practical green synthetic route for the preparation of magnetic recyclable core-shell nanocatalyst that can be a good candidate for the treatment of organic contaminants in wastewater adhering to green chemistry principles for the environmental pollution concerns.

Key words: Magnetic recyclable nanocatalyst, *Epilobium parviflorum,* silver nanoparticle, heterogeneous catalyst, reduction of organic dyes

1. Introduction

Organic dye contaminants have become an acute concern and problem in the environment due to their release or discharge into the environment as arising intensive activities of different chemical industries, including food, textile, cosmetics, plastics, paint, and indeed domestic waste [1,2]. Most of these waste dyestuffs or effluents are toxic, carcinogenic, and even mutagenic, as well as posing serious risks to living organisms, especially to human health [3–6]. Although diverse techniques involving adsorption, precipitation, photocatalytic degradation, and advanced oxidation processes (AOPs) have been introduced to treat organic dye pollutants up to now, they could be most frequently time-consuming, impractical, and expensive [7–9]. For these reasons, there has been still a growing interest to develop methods or strategies for the removal of dye pollutants before their release from various industries into the environment.

Based on this purpose, metal nanoparticles with higher Fermi potential that enable them to catalyze electron transfer reaction with lowered reduction potential have attracted great interest in reducing organic dye pollutants [10,11]. In particular, silver nanoparticles (AgNPs) among several noble metal-based catalysts containing gold, palladium, and platinum have gained significant research and application for a variety of catalytic reactions, some of which are reduction of organic compounds, selective oxidation, and NO$_x$ reduction, because of their unique properties, including low-cost, high optical, catalytic, and antibacterial properties [12,13]. In this point, not only the use of reducing agents in the production of AgNPs might lead to environmental toxicity and biohazards but also because the industry promotes catalytic processes with ease operation, employ and recyclability, the use of green synthetic roots and environment in preparing a heterogeneous catalyst remains among the main research principles [14,15]. For this reason, magnetic nanoparticles (MNPs) have received much interest in the heterogeneous catalyst as a useful support owing to their ease of separation from the reaction media using an external magnetic field compared to filtration and centrifugation processes, high dispersion, and recyclability [16–18]. Therefore, MNPs can improve the separation and recovery of AgNPs from the reaction media.

Among different coating materials, silica as a protective shell can be facilitated to maintain the stability of MNPs and prevent their interaction with complex matrices with the desired stability [19,20]. In addition, plant-mediated synthesis of nanoparticles has attracted great attention depending on its several advantages, comprising non-toxic, safe, cost

*Correspondence: gelmaci@adiyaman.edu.tr

effective, especially being environmentally friendly [21–24]. Thus, the aforementioned environmental concerns can be overcome in the fast and economic production of magnetic core-shell nanoparticles with more stable properties via the immobilization of silver nanoparticles on silica coated MNPs by using plant extracts as reducing agents.

In our previous study, we have introduced *Epilobium parviflorum* (*EP*) extract as a novel reducing, stabilizing agent, and coating material for the preparation of Ag immobilized nanocatalyst using manganese ferrite magnetic core as an alternative to commonly used Fe_3O_4 core supports [25]. Apart from this study, we addressed herein the green and successful preparation technique for the synthesis of highly stable $MnFe_2O_4$@SiO_2-Ag core-shell magnetically recyclable nanocatalyst using *EP* extract for the first time. In this perspective, the current research has come to a focal point as the used *EP* extracts serve on the basis of the green synthesis of heterogeneous catalyst without using any additional chemicals, stabilizer, surfactant, toxic or extra reducing agents, and become inspiring for the future studied dealing with more environmental concerns. The $MnFe_2O_4$@SiO_2-Ag has also been investigated as a useful catalyst in the reduction of some organic pollutant dyes.

2. Materials and methods
2.1. Chemicals and materials
Iron (III) chloride hexahydrate ($FeCl_3.6H_2O$), manganese (II) chloride tetrahydrate ($MnCl_2.4H_2O$), ammonia (NH_3), silver nitrate ($AgNO_3$), polyvinylpyrrolidone (PVP), methylene blue (MB), and rhodamine B (RhB) were purchased from Sigma-Aldrich and used without any further purifications. *Epilobium parviflorum* (EP) plant (green tea extract) was purchased from the local market in Turkey.

2.2. Instrumentation
A Pan Analytical Empyrean diffractometer with a PixCell3D detector was used for the Powder X-ray diffraction pattern (XRD) measurements. Attenuated total reflectance-Fourier transform infrared spectroscopy (ATR-FTIR) spectra were collected between the wavelength range of 600–4000 cm^{-1} via PerkinElmer Spectrum 100 FT-IR Spectrometer. The water content of the samples was detected using TA Instrument (New Castle, DE) thermal analysis system with a heating program of 10 °C min^{-1} under air flow (100 mL min^{-1}) by thermogravimetry. The morphological analyses were carried out using an electron microscope (SEM, ZEISS Sigma 300) integrated with energy-dispersive X-ray spectroscopy (EDS), and high contrast transmission electron microscope (TEM, Hitachi HT7700 with EXALENS). UV-Vis measurements were carried out via a Carry 60 UV-Vis spectrometer, (Agilent, USA) with a 1 cm quartz cell.

2.3. Synthesis of $MnFe_2O_4$ nanoparticles
A mixture of Iron (III) chloride hexahydrate ($FeCl_3.6H_2O$) (6.5 g) and manganese (II) chloride tetrahydrate ($MnCl_2.4H_2O$) (4.0 g), and 0.2 g polyvinylpyrrolidone (PVP) in 80 mL of de-ionized water (100 mL) was stirred vigorously for 3 h. Afterwards, 20 mL of 0.1M NH_4OH solution was slowly added and irradiated under microwave for 20 min at 100 °C. After cooling the reaction mixture to room temperature, the black precipitate of $MnFe_2O_4$ nanoparticles were separated magnetically and washed three times with mixture of ethanol-deionized water [25].

2.4. Synthesis of $MnFe_2O_4$@SiO_2 core-shell nanoparticles
Synthesis of $MnFe_2O_4$@SiO_2 core-shell nanoparticles were simply adopted from the literature [20]. In summary, 1.0 g of $MnFe_2O_4$ nanoparticles were added to a solution of 5.0 mL of NH_4OH (25%) and 200.0 mL of ethanol and dispersed well. 2.5 mL of tetraethyl orthosilicate was added over the resulting mixture dropwise while vigorously stirring. After stirring the mixture for 12 h at 40 °C, the obtained $MnFe_2O_4$@SiO_2 nanoparticles were separated using an external magnet, washed several times with ethanol, and dried at room temperature.

2.5. Synthesis of $MnFe_2O_4$@SiO_2 -Ag
The preparation of *EP* green tea extract was reported in our recent study [26]. For further synthesis of the $MnFe_2O_4$@SiO_2-Ag nanocatalyst, 50 mg of $MnFe_2O_4$@SiO_2 was added over a stirring solution of 50.0 mL of $AgNO_3$ (0.15 mM) and dispersed well. Afterwards, 8.0 mL of the *EP* extract was added while constant stirring at 50 °C for 60 min. After cooling the reaction mixture to room temperature, the precipitates were collected by using a niobium magnet and washed several times with distilled water and, later on, with three times with ethanol to get rid of impurities [20].

2.6. Catalytic activity of $MnFe_2O_4$@SiO_2-Ag
The catalytic performance of $MnFe_2O_4$@SiO_2-Ag was tested over the reduction reaction of RhB and MB by $NaBH_4$. Prior to the catalytic reactions, in order to completely achieve adsorption-desorption equilibrium, the $MnFe_2O_4$@SiO_2-Ag NPs (20 μL, 2.15 mg mL^{-1}), de-ionized water (0.75 mL), and RhB (40 μL, 3.06 mM) were stirred for 30 min. After that, 2.25

mL portion of the 0.1 M NaBH$_4$ was poured into this solution. By adopting the same procedure, the catalytic assays were completed by using MB (10 µL, 2.25 mM) and NaBH$_4$ (2.25 mL, 0.1 M). UV-Vis measurements were recorded between the range of 350–700 nm and 500–750 nm for RhB ((λ_{max} = 554 nm) and MB (λ_{max} = 670 nm) to monitor the performed reaction until bleaching the color of the aqueous solutions of dyes.

3. Results and discussion

3.1. Synthesis and characterization

In the nanocomposite catalyst design, MnFe$_2$O$_4$ was chosen as it has high saturation magnetization value and rough surface [17]. Then, the MnFe$_2$O$_4$ surface was coated with SiO$_2$ thin layer to prevent agglomeration and create a porous area [27]. The facility of the *EP* green tea extract for the reduction and stabilization of metal nanoparticles as coating material with its rich content in terms of phenolic compound derivatives such as tannins, flavonoids, and phenolic acids has been demonstrated in our recent study [25]. Considering this potential of *EP* extracts, herein, we employed them as efficient reducing agents for the immobilization of AgNPs on the protective SiO$_2$ outer layer. Therefore, the resulting MnFe$_2$O$_4$@SiO$_2$-Ag nanocomposite can be used as a low-cost, recyclable, environmentally friendly, and active catalyst platform. The experimental strategy for the preparation of MnFe$_2$O$_4$@SiO$_2$-Ag was illustrated in Scheme 1. The MnFe$_2$O$_4$@SiO$_2$-Ag was synthesized in two-step approach. In the first step, the silica layer was coated on the magnetic core nanoparticle, MnFe$_2$O$_4$. In the next step, silver ions was adsorbed and *in situ* reduced on the surface of the MnFe$_2$O$_4$@SiO$_2$ core-shell nanospheres by means of *EP* green tea extract in aqueous solution without using any other organic solvent, stabilizing, or reducing agents.

The crystalline phase, morphology, and particle size of the as prepared MnFe$_2$O$_4$@SiO$_2$-Ag samples were examined via X-ray diffraction (XRD), Scanning Electron Microscopy (SEM), and Transmission Electron Microscopy (TEM). Figure 1 a shows the XRD patterns of MnFe$_2$O$_4$ nanoparticles. The spinel MnFe$_2$O$_4$ displayed peaks at 2θ values of 18.3° (111), 30.2° (220), 35.5° (311), 43.1° (400), 53.5° (422), 57.1° (511), and 62.6° (440), which can be indexed to the JCPDS 17-465 [28,29]. The SEM image of MnFe$_2$O$_4$ shows aggregates of well-defined spherical-like particles of sizes between 100–150 nm (Figure 1b).

The SEM micrographs of MnFe$_2$O$_4$@SiO$_2$ and MnFe$_2$O$_4$@SiO$_2$-Ag core-shell NPs are shown in Figures 2a–2d. In the current study, SiO$_2$ thin layer was coated on the surface of MnFe$_2$O$_4$ magnetic core by hydrolysis of TEOS [30,31]. The SEM image of MnFe$_2$O$_4$@SiO$_2$ showed that the MnFe$_2$O$_4$ core was homogeneously and successfully coated with SiO$_2$ layer. The detailed core-shell structure was further confirmed by high-resolution TEM image (Figure 2b, 2c) and EDS (Figure 2d). It can be seen from Figure 2e that an amorphous SiO$_2$ layer with a thickness of ~20 nm was homogeneously distributed over the surface of MnFe$_2$O$_4$. Moreover, The EDS analysis of MnFe$_2$O$_4$@SiO$_2$-Ag clearly displayed signals from Ag, Mn, Fe, and Si atoms (Figure 2d). In this point, our previous study confirms that AgNPs are formed as a result of the *in situ* upon oxidation of active phenolic functional groups and derivatives in the *EP* extract by Ag$^+$ ions at neutral pH value [25]. The resulting AgNPs were observed in spherical shape with 15 nm of average particle size in TEM analysis (Figure 2e, 2f). These results suggest that the AgNPs could be formed in every layer of the SiO$_2$ layer. Thus, porous outer shell coated on the magnetic support can create a platform for the acceleration of mass-energy transfer to active catalysts such as Ag, Au, Pd, etc. [32,33].
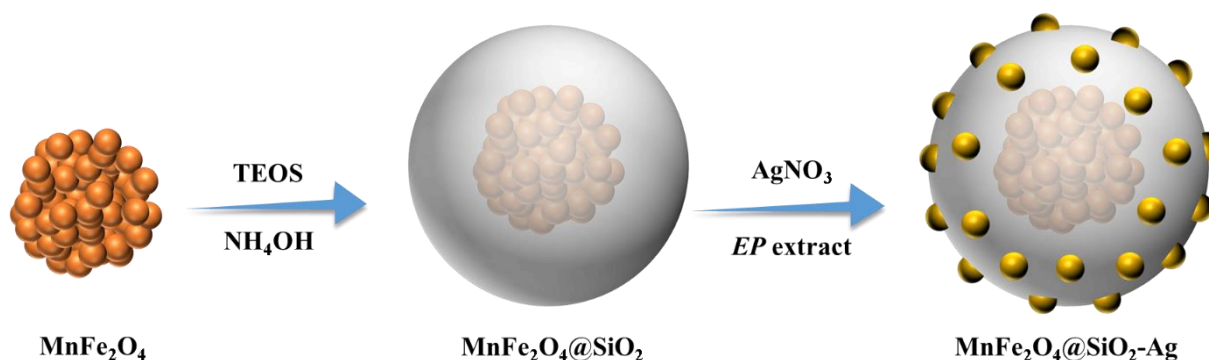
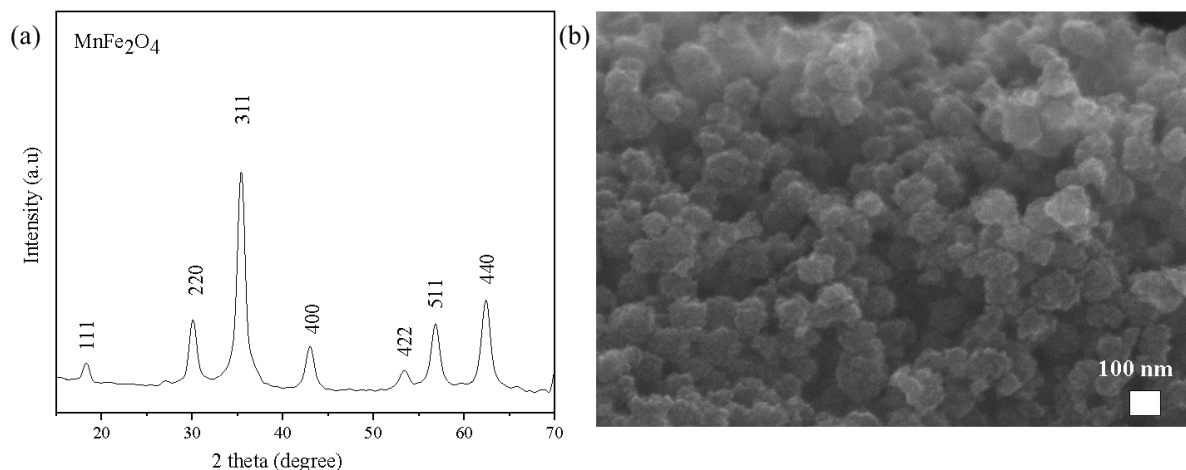**Scheme 1.** Systematic synthetic route for the production of MnFe$_2$O$_4$@SiO$_2$-Ag nanocatalyst.

Figure 1. X-ray diffraction pattern (a) and SEM image of $MnFe_2O_4$ (b).

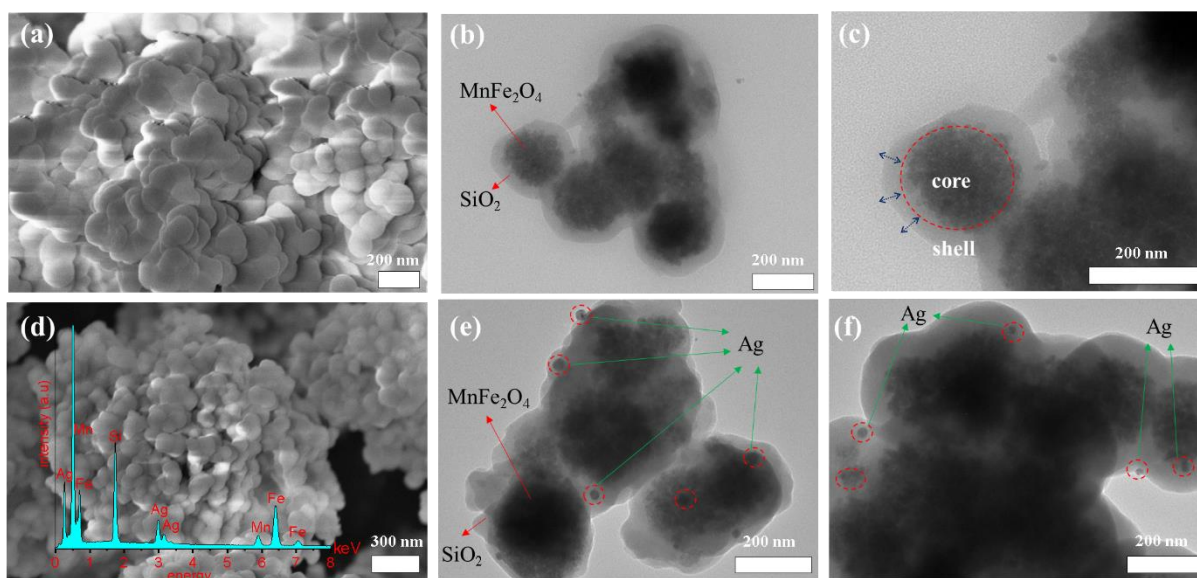**Figure 2.** SEM image of $MnFe_2O_4@SiO_2$ core-shell NPs (a). TEM image of $MnFe_2O_4@SiO_2$ core-shell NPs (b, c). SEM image and Energy Dispersive Spectroscopy (EDS) analysis of $MnFe_2O_4@SiO_2$-Ag core-shell NPs (d). TEM image of $MnFe_2O_4@SiO_2$-Ag core-shell NPs (e, f).

XRD patterns of the $MnFe_2O_4@SiO_2$-Ag contain peaks of both crystalline $MnFe_2O_4$ and AgNPs (Figure 3a). The sharp diffraction peaks at $2\theta = 38.2°$, $44.3°$, $64.5°$ and $76°$ can be indexed to the reflections of the (111), (200) and (220) crystalline planes of face-centered-cubic Ag (JCPDS card no. 04-0783), respectively [25]. In order to further confirm the composition and structure of the $MnFe_2O_4@SiO_2$-Ag, thermal stability was investigated. A mass loss of $MnFe_2O_4$ is 5% up to 280 °C due to the volatilization of physically absorbed water and residual organic surfactant. As for $MnFe_2O_4@SiO_2$-Ag, the mass loss is 1% higher than that of $MnFe_2O_4$ due to the decomposition of the thin layer of SiO_2 [34] (Figure 3b).

The low recovery costs of catalysts are a significant factor in the development of sustainable catalyst systems [35–41]. Therefore, magnetically supported catalyst systems are considered to be one of the most important platforms as they can be easily separated from the reaction media via the aid of an external magnet [28,42,43]. Magnetic properties of the obtained catalysts were elucidated with vibrating sample magnetometer (VSM) analyzer between the range of -20000 Oe +20000 Oe at room temperature. The magnetization saturation values (Ms) of $MnFe_2O_4$ is 52.12 emu g^{-1}. However, the saturation magnetization of the silica-coated and Ag loaded $MnFe_2O_4@SiO_2$-Ag NPs decreases as the silica shell thickness increases, and it has value of $\sim$33.51 emu g^{-1} with shell thickness of 20 nm, respectively (Figure 3c).
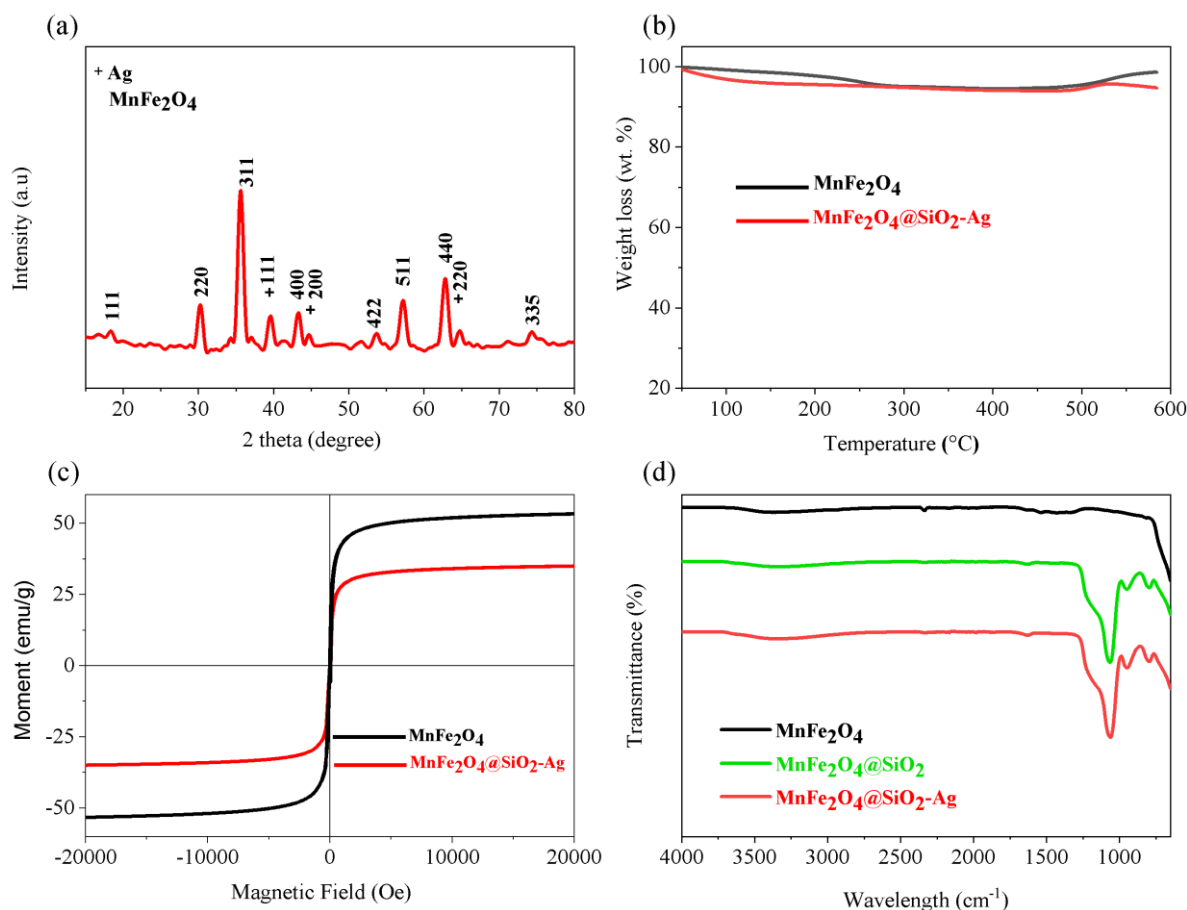
Figure 3. X-ray diffraction pattern of MnFe$_2$O$_4$@SiO$_2$-Ag (a), TGA curves of MnFe$_2$O$_4$ and MnFe$_2$O$_4$@SiO$_2$-Ag (b), Magnetic curves of MnFe$_2$O$_4$ and MnFe$_2$O$_4$@SiO$_2$-Ag (c), ATR-FTIR spectra of MnFe$_2$O$_4$ and MnFe$_2$O$_4$@SiO$_2$-Ag (d).

ATR-FTIR spectroscopy was also used to monitor the SiO$_2$ coating process of the MnFe$_2$O$_4$ surface and the Ag doping process with green synthesis [34,44]. The ATR-FTIR spectrum of   MnFe$_2$O$_4$@SiO$_2$ exhibits a broad band in the region 3400 cm^{-1} and fewer intense band at 1650 cm^{-1}, which are due to O-H stretching and O-H deformation vibrations of coordinated water, respectively (Figure 3d) [45]. These O-H bands also include Si-OH stretchings and vibrations of SiO$_2$. The bands centered at 1090 cm^{-1} and 810 cm^{-1} are, respectively, assigned to the vibrations of Si-O-Si (asym) and the vibration of Si-O-Si (sym) [46]. No significant change was observed in the ATR-FTIR spectra of MnFe$_2$O$_4$@SiO$_2$-Ag on doping with AgNPs except minor intensity and position changes in the ~750–1250 cm^{-1} region. These results show that Ag nanoparticles formed by reduction with green tea extract do not cause deformation on the SiO$_2$ surface.

3.2. Catalytic properties of MnFe$_2$O$_4$@SiO$_2$-Ag

Over the last decade, industrial effluents bearing organic dye pollutants and stemming from various activities such as textile, plastic, cosmetic and have come to a serious problem to be overcome [47]. Due to their water solubility to some extend up to 10–200 mg/L, dye contaminants are regarded as one of the most important resources of the water pollution all over the world [48]. In spite of numerous methods, involving precipitation, adsorption or biogenic treatment have been employed; the concerns still maintain due to their high cost, generation of inadmissible side products that might lead to damages on animal and human, comprising of liver, kidney, etc. [47], and requisition of possible high-energy demands, especially in massive treatments [49]. Therefore, the complete removal of the organic pollutants from the industrial effluents by direct catalytic reductions has been occurring as a major environmentally friendly remedy [50].

Former studies have shown that AgNPs exhibited good catalytic activity and selectivity for various reactions [40,51,52]. In the present study, the catalytic performance of the green synthesized MnFe$_2$O$_4$@SiO$_2$-Ag nanocatalyst by using *EP* extract was evaluated in the model direct reduction reactions of MB and RhB by NaBH$_4$, as they are good representative members of the hazardous organic pollutants [53,54]. In addition, their decolorization processes can be easily monitored by naked eye and UV-Vis spectroscopy from the unique absorption bands at around 554 and 670 nm

for RhB and MB, respectively [55,56]. Thus, the practical investigation of the degradation of MB and RhB could be beneficial for the purification of dye effluents. As it can be observed from Figures 4a and 4b, conversions of dyes were completed in 7.39 min (MB) and 13.13 min (RhB) after addition of the $MnFe_2O_4@SiO_2$-Ag nanocatalyst to the individual solutions, including the excess amount of $NaBH_4$. The color bleaching of the aqueous solutions together with the leveling off the UV-Vis bands after gradual decreases were also indicated the completion of the reduction reactions successfully. These results confirmed the successful degradation of MB and RhB to their leuco forms [34,57–60] by means of the redox reactions appearing on the surface of the electron relay systems (AgNPs) enabling the transfer of surface hydride ion electrons from BH_4^- to the target acceptor dyes MB and RhB [48,60,61]. Possible reduction mechanism of the MB and RhB by $MnFe_2O_4@SiO_2$-Ag was illustrated in Scheme 2. Taken into consideration the above results, it can be concluded that chromophore functional groups of C=N- and -N=N- present in MB and RhB have been successfully reduced to those of colorless C-N and N-N in the presence of immobilized AgNPs on the $MnFe_2O_4@SiO_2$ surface [62,63].

In order to enlighten the catalytic role of the as synthesized nanocatalyst on diverse organic pollutants, rate constants for the MB and RhB reduction reactions were calculated and compared in Figure 4c. During the catalytic reduction studies, the concentration of the $NaBH_4$ was used as excessively higher than the used dyes in order to obey the pseudo first-order kinetics described by $ln (A_t /A_0) = - kt,$ where $k, t, A_t,$ and A_0 correspond to apparent rate constant, reaction time, absorbances of dyes at time "t" and "0", respectively [64]. The obtained results revealed that the $MnFe_2O_4@SiO_2$-Ag exhibited higher catalytic towards MB (0.3 min^{-1}) than RhB (0.07 min^{-1}) (Figure 4c). To further get a better insight into the catalytic activity of the $MnFe_2O_4@SiO_2$-Ag and show the facility of this work, normalized rate constants (k_{nor}=k/m, where the m is the catalyst mass) were calculated [65], and the performance of our catalyst was compared with the other catalyst systems in the literature. The results were summarized in Table. Compared with the other various metal-based catalyst systems, the catalytic activity of the green synthesized $MnFe_2O_4@SiO_2$-Ag was distinctive and even satisfactory with the k_{nor} values of 116.28 s^{-1} g^{-1} and 27.13 s^{-1} g^{-1} for MB and RhB, respectively. Therefore, it could be inferred that the $MnFe_2O_4@SiO_2$-Ag nanocatalyst can be utilized with a good potential for the reduction of dye contaminants in water and be promising to future studies with its environmentally friendly preparation process by *EP* extract without using extra reducing or stabilizing agent that might be toxic for the living organism and the environment.

3.3. Recyclability of the $MnFe_2O_4@SiO_2$-Ag

The recyclability and stability of the catalyst are important factors to show the sustainability of the core-shell magnetic nanocatalysts prepared by using *EP* extract for the immobilization of AgNPs on the $MnFe_2O_4@SiO_2$ surface. Thus, the recyclability tests were conducted on the model reduction reaction of RhB by $NaBH_4$ in the presence of the $MnFe_2O_4@SiO_2$-Ag, and the obtained results were presented in Figure 4d. For a routine cyclic test, an external niobium magnet was used to separate the used nanocatalyst from the reaction media after the catalytic degradation. Before starting the subsequent cycle, the recycled nanocatalyst was washed several times with water and subsequently three times with ethanol. After dried under vacuum, they were used for the next cycle. In each cycle, the same procedure was repeated. Figure 4d shows the recyclability test results. In the formation of these graphs, the maximum absorbance
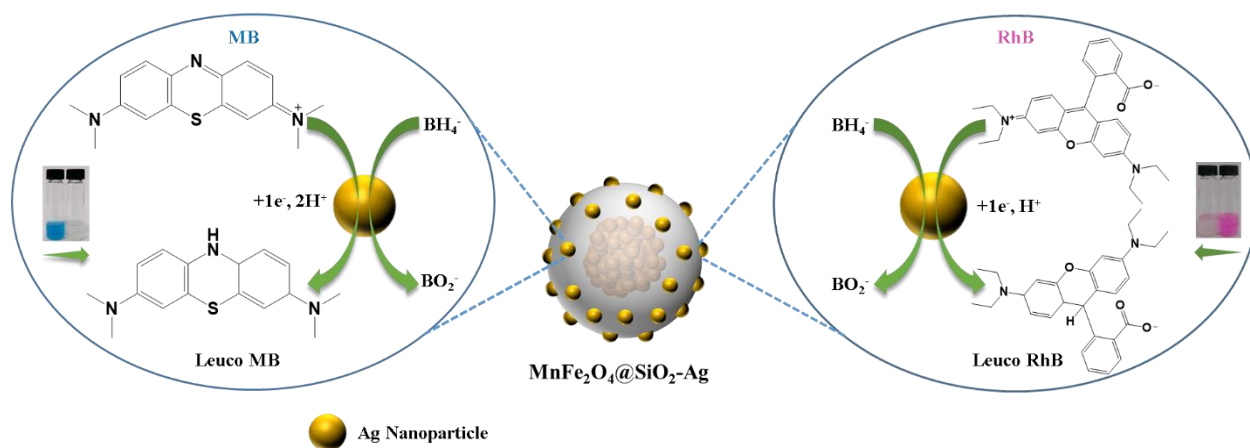
Scheme 2. Possible mechanism of the reduction of MB and RhB catalyzed by $MnFe_2O_4@SiO_2$-Ag.

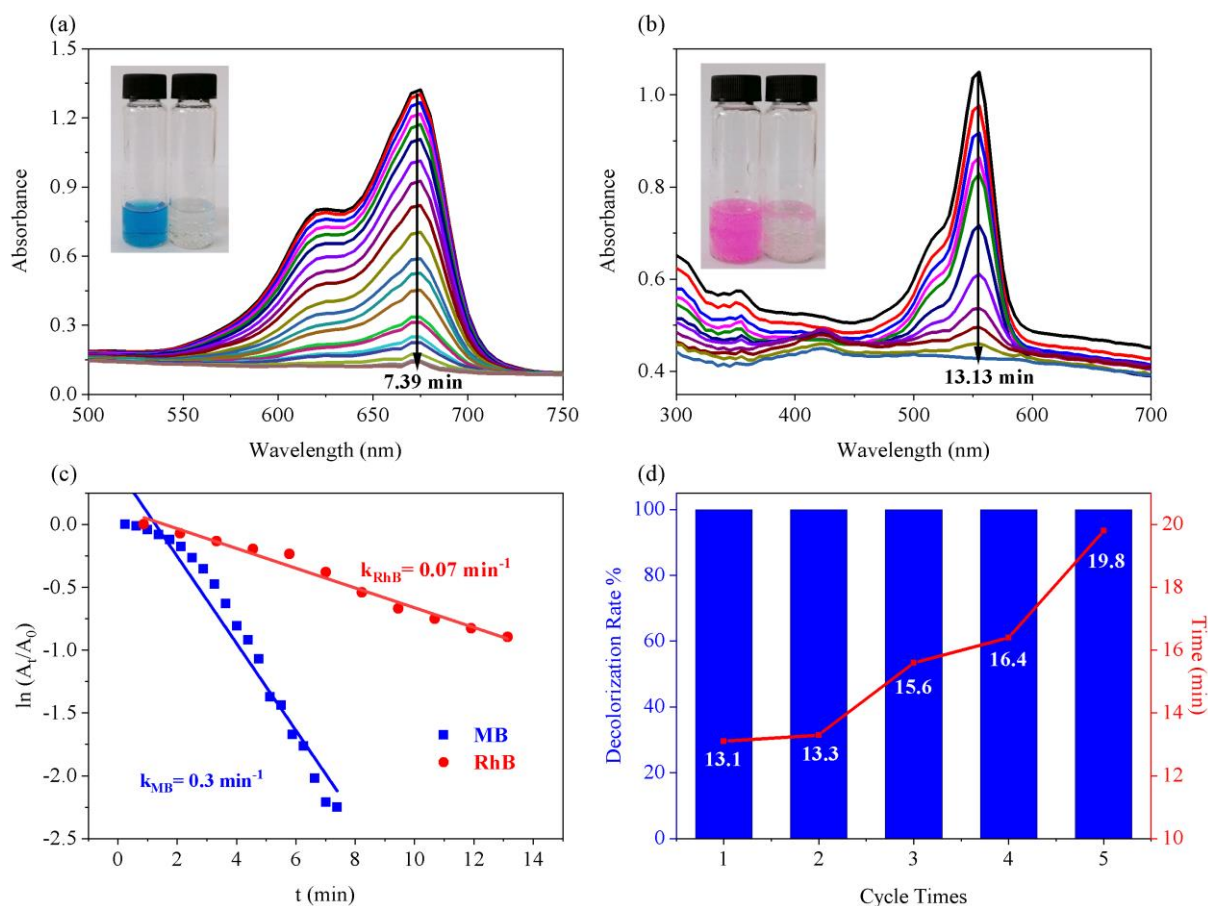**Figure 4.** The reduction of MB (a) and RhB (b) in aqueous solution using MnFe$_2$O$_4$@SiO$_2$-Ag nanocatalyst. The comparison of the first-order kinetic plots of MB and RhB in the presence of MnFe$_2$O$_4$@SiO$_2$-Ag (c). Recycling of the MnFe$_2$O$_4$@SiO$_2$-Ag for the reduction of RhB by NaBH$_4$ (d).

Table. Comparison of the catalytic performances of MnFe$_2$O$_4$@SiO$_2$-Ag with other catalyst system over MB and 4-NP reduction by NaBH$_4$.

Dyes	Catalyst system	Catalyst mass (mg)	k (10^{-3} s^{-1})	k$_{app}$ (s^{-1} g^{-1})	Time (min)	Ref.
MB	AgNPs	0.5	5.75	11.50	12	[66]
	Fe$_3$O$_4$@Ag	1.6	6.83	4.27	6	[67]
	MGO-PDA@Ag	3.0	7.12	2.37	7	[68]
	Ag/PSNM-3	2.0	2.23	1.12	11	[69]
	Fe$_3$O$_4$@HA@Ag	1	1.33	1.33	20	[70]
	Fe$_3$O$_4$@His@Ag	1	4.50	4.50	4	[71]
	MnFe$_2$O$_4$@SiO$_2$-Ag	0.043	5.00	116.28	7.39	This work
RhB	Ag/TP	10	5.68	0.57	6	[72]
	Fe$_3$O$_4$@EDTA-Ag	30	34.00	1.13	3	[73]
	Fe$_3$O$_4$@Nico-Ag	1	3.83	3.83	10	[74]
	MnFe$_2$O$_4$@EP@Ag	0.0214	7.50	350.47	7.63	[25]
	AgCl@TA5.0-cellulose hydrogels	1	32.30	32.30	3	[75]
	MnFe$_2$O$_4$@SiO$_2$-Ag	0.043	1.17	27.13	13.13	This work

values of the RhB were used to calculate percent decolorization rates. This overlapped plot drawn from the decolorization rate % and time (min) proves that the MnFe$_2$O$_4$@SiO$_2$-Ag maintains its catalytic activity through the five repeated cycles without any loss in its decolorization efficiency (100%), so that the possibility of leaching AgNPs from the MnFe$_2$O$_4$@SiO$_2$-Ag nanocomposites were ignored. Nevertheless, it can be also seen from Fig 4d that time required to complete the

reaction in each cycle increases from 13.1 min (first cycle) to 19.8 min (fifth cycle). This increase could be attributed to loss of magnetic catalyst during the recovery process of the catalyst [65]. Overall, the produced $MnFe_2O_4@SiO_2$-Ag core-shell magnetic nanocatalyst were stable and sufficient enough for the reduction of RhB, and they could be good candidates and have a great potential for the removal of dye contaminants in water.

4. Conclusion
In the current study, we showed a green synthetic strategy for the immobilization of AgNPs on manganese ferrite nanoparticles coated with the protective silica layer by using *EP* extract without facilitating any other reducing or stabilizing agents. This approach presents significant advantages over the existing ones in terms of using mild reaction conditions, requiring no extra reducing agent or surfactant, organic solvent, and hazardous materials. Bio-based process used here does not generate environmentally hazardous waste. For this reason, the reaction product occurring in these processes do not frequently need purification. The prepared catalyst system in this study revealed sufficient catalytic activity for the removal of MB and RhB compared with the previous studies. Moreover, the superior magnetization characteristics of the $MnFe_2O_4@SiO_2$-Ag led them to be used several times without losing a prominent catalytic activity in each successive cycle. Thus, the obtained overall results suggest that the $MnFe_2O_4@SiO_2$-Ag core-shell magnetic nanocomposites could be highly efficient and stable catalytic systems for the treatment of organic or dye contaminants and numerous applications in heterogeneous catalysis considering the environmental pollution concerns.

Authors' contributions
Gökhan Elmacı: Conceptualization, formal analysis, investigation, methodology, software, validation, visualization. Ali Serol Ertürk: Conceptualization, formal analysis, investigation, methodology, resources, software, validation, visualization, writing-original draft, writing-review & editing. Mustafa Ulvi Gürbüz: Data curation, formal analysis, investigation, methodology, validation, visualization.

Data availability
The datasets used and/or analyzed during the current study are available from the corresponding author on reasonable request.

References

1. Mani S, Chowdhary P, Bharagava RN. Textile wastewater dyes: Toxicity profile and treatment approaches. Emerging and eco-friendly approaches for waste management 2018; 219-244. doi: 10.1007/978-981-10-8669-4_11

2. Mondal P, Baksi S, Bose D. Study of Environmental Issues in Textile Industries and Recent Wastewater Treatment Technology. World Scientific News 2017; 61: 98-109.

3. Crini G. Studies on adsorption of dyes on beta-cyclodextrin polymer. Bioresource Technology 2003; 90 (2): 193–198. doi: 10.1016/S0960-8524(03)00111-1

4. Wijetunga S, Li X-F, Jian C. Effect of organic load on decolourization of textile wastewater containing acid dyes in upflow anaerobic sludge blanket reactor. Journal of Hazardous Materials 2010; 177 (1-3): 792–798. doi: 10.1016/j.jhazmat.2009.12.103

5. Kavimani T, Senthilkumar PL. Anaerobic Treatment of Dye Wastewater using Upflow Anaerobic Sludge Blanket Reactor. International Journal of Innovative Technology and Exploring Engineering 2019; 8 (12): 3178–3181. doi: 10.35940/ijitee.L3044.1081219

6. Ertürk AS. PAMAM dendrimer-enhanced removal of cobalt ions based on multiple-response optimization using response surface methodology. Journal of the Iranian Chemical Society 2018; 15 (8): 1685–1698. doi: 10.1007/s13738-018-1366-3

7. Ambashta RD, Sillanpää M. Water purification using magnetic assistance: A review. Journal of Hazardous Materials 2010; 180 (1-3): 38–49. doi: 10.1016/j.jhazmat.2010.04.105

8. Chan SHS, Yeong Wu T, Juan JC, Teh CY. Recent developments of metal oxide semiconductors as photocatalysts in advanced oxidation processes (AOPs) for treatment of dye waste-water. Journal of Chemical Technology & Biotechnology 2011; 86 (9): 1130–1158. doi: 10.1002/jctb.2636

9. Burakov AE, Galunin EV, Burakova IV, Kucherova AE, Agarwal S et al. Adsorption of heavy metals on conventional and nanostructured materials for wastewater treatment purposes: A review. Ecotoxicology and Environmental Safety 2018; 148: 702–712. doi: 10.1016/j.ecoenv.2017.11.034

10. Jana NR, Wang ZL, Pal T. Redox Catalytic Properties of Palladium Nanoparticles: Surfactant and Electron Donor–Acceptor Effects. Langmuir 2000; 16 (6): 2457–2463. doi: 10.1021/la990507r

11. Jana NR, Pal T. Redox Catalytic Property of Still-Growing and Final Palladium Particles: A Comparative Study. Langmuir 1999; 15 (10): 3458–3463. doi: 10.1021/la981512i

12. Shimizu K, Sawabe K, Satsuma A. Unique catalytic features of Ag nanoclusters for selective NOx reduction and green chemical reactions. Catalysis Science & Technology 2011; 1 (3): 331-341. doi: 10.1039/c0cy00077a

13. Holmes AB, Gu FX. Emerging nanomaterials for the application of selenium removal for wastewater treatment. Environmental Science: Nano 2016; 3 (5): 982–996. doi: 10.1039/C6EN00144K

14. Nasrollahzadeh M, Mohammad Sajadi S, Rostami-Vartooni A, Khalaj M. Green synthesis of Pd/Fe 3 O 4 nanoparticles using Euphorbia condylocarpa M. bieb root extract and their catalytic applications as magnetically recoverable and stable recyclable catalysts for the phosphine-free Sonogashira and Suzuki coupling reactions. Journal of Molecular Catalysis A: Chemical 2015; 396: 31–39. doi: 10.1016/j.molcata.2014.09.029

15. Veisi H, Gholami J, Ueda H, Mohammadi P, Noroozi M. Magnetically palladium catalyst stabilized by diaminoglyoxime-functionalized magnetic Fe_3O_4 nanoparticles as active and reusable catalyst for Suzuki coupling reactions. Journal of Molecular Catalysis A: Chemical 2015; 396: 216–223. doi: 10.1016/j.molcata.2014.10.012

16. Baig RBN, Varma RS. Magnetically retrievable catalysts for organic synthesis. Chemical Communications 2013; 49: 752–770. doi: 10.1039/C2CC35663E

17. Ertürk AS, Elmacı G. PAMAM Dendrimer Functionalized Manganese Ferrite Magnetic Nanoparticles: Microwave-Assisted Synthesis and Characterization. Journal of Inorganic and Organometallic Polymers and Materials 2018; 28 (5): 2100–2107. doi: 10.1007/s10904-018-0865-0

18. Bonyasi F, Hekmati M, Veisi H. Preparation of core/shell nanostructure Fe3O4@PEG400-SO3H as heterogeneous and magnetically recyclable nanocatalyst for one-pot synthesis of substituted pyrroles by Paal-Knorr reaction at room temperature. Journal of Colloid and Interface Science 2017; 496: 177–187. doi: 10.1016/j.jcis.2017.02.023

19. Deng Y-H, Wang C-C, Hu J-H, Yang W-L, Fu S-K. Investigation of formation of silica-coated magnetite nanoparticles via sol–gel approach. Colloids and Surfaces A: Physicochemical and Engineering Aspects 2005; 262 (1-3): 87–93. doi: 10.1016/j.colsurfa.2005.04.009

20. Mohammadi P, Sheibani H. Green synthesis of Fe3O4@SiO2 -Ag magnetic nanocatalyst using safflower extract and its application as recoverable catalyst for reduction of dye pollutants in water. Applied Organometallic Chemistry 2018; 32 (4): e4249. doi: 10.1002/aoc.4249

21. Balentine DA, Wiseman SA, Bouwens LCM. The chemistry of tea flavonoids. Critical Reviews in Food Science and Nutrition 1997; 37 (8): 693–704. doi: 10.1080/10408399709527797

22. Graham HN. Green tea composition, consumption, and polyphenol chemistry. Preventive Medicine 1992; 21 (3): 334–350. doi: 10.1016/0091-7435(92)90041-F

23. Veisi H, Ghorbani F. Iron oxide nanoparticles coated with green tea extract as a novel magnetite reductant and stabilizer sorbent for silver ions: Synthetic application of Fe3O4@green tea/Ag nanoparticles as magnetically separable and reusable nanocatalyst for reduction of 4-nitrophenol. Applied Organometallic Chemistry 2017; 31 (10): e3711. doi: 10.1002/aoc.3711

24. Ertürk AS. Controlled Production of Monodisperse Plant-Mediated AgNP Catalysts Using Microwave Chemistry: A Desirability-Function-Based Multiple-Response Optimization Approach. ChemistrySelect 2019; 4 (32): 9300–9308. doi: 10.1002/slct.201902197

25. Gürbüz MU, Koca M, Elmacı G, Ertürk AS. In situ green synthesis of MnFe2O4@EP@Ag nanocomposites using Epilobium parviflorum green tea extract: An efficient magnetically recyclable catalyst for the reduction of hazardous organic dyes. Applied Organometallic Chemistry 2021; 35(6): e6230. doi: 10.1002/aoc.6230

26. Ertürk AS. Biosynthesis of Silver Nanoparticles Using Epilobium parviflorum Green Tea Extract: Analytical Applications to Colorimetric Detection of Hg2+ Ions and Reduction of Hazardous Organic Dyes. Journal Cluster Science 2019; 30 (5): 1363–1373. doi: 10.1007/s10876-019-01634-4

27. Maklakov SS, Lagarkov AN, Maklakov SA, Adamovich YA, Petrov DA et al. Corrosion-resistive magnetic powder Fe@SiO2 for microwave applications. Journal of alloys and compounds 2017; 706: 267-273. doi: 10.1016/j.jallcom.2017.02.250

28. Kayili HM, Ertürk AS, Elmacı G, Salih B. Poly(amidoamine) dendrimer-coated magnetic nanoparticles for the fast purification and selective enrichment of glycopeptides and glycans. Journal of Separation Science 2019; 42 (20): 3209–3216. doi: 10.1002/jssc.201900492

29. Elmaci G, Frey CE, Kurz P, Zümreoğlu-Karan B. Water oxidation catalysis by using nano-manganese ferrite supported 1D-(tunnelled), 2D-(layered) and 3D-(spinel) manganese oxides. Journal of Materials Chemistry A 2016; 4 (22): 8812–8821. doi: 10.1039/c6ta00593d

30. De G, Karmakar B, Ganguli D. Hydrolysis-condensation reactions of TEOS in the presence of acetic acid leading to the generation of glass-like silica microspheres in solution at room temperature. Journal of Materials Chemistry 2000; 10 (10): 2289-2293. doi: 10.1039/b003221m

31. Karmakar B, De G, Ganguli D. Dense silica microspheres from organic and inorganic acid hydrolysis of TEOS. Journal of Non-crystalline Solids 2000; 272 (2-3): 119-126. doi: 10.1016/S0022-3093(00)00231-3.

32. Yang J. Noble metal-based nanocomposites: Preparation and applications. Weinheim, Germany: John Wiley & Sons, 2019. doi: 10.1002/9783527814305

33. Gawande MB, Goswami A, Asefa T, Guo H, Biradar AV et al. Core-shell nanoparticles: synthesis and applications in catalysis and electrocatalysis. Chemical Society Reviews 2015; 44 (21): 7540-7590. doi: 10.1039/c5cs00343a

34. Kurtan U, Amir M, Yildiz A, Baykal A. Synthesis of magnetically recyclable MnFe2O4 @SiO 2 @Ag nanocatalyst: Its high catalytic performances for azo dyes and nitro compounds reduction. Applied Surface Science 2016; 376: 16–25. doi: 10.1016/j.apsusc.2016.02.120

35. Meral K, Metin Ö. Graphene oxide{magnetite nanocomposite as an effcient and magnetically separable adsorbent for methylene blue removal from aqueous solution. Turkish Journal of Chemistry 2014; 38 (5): 775–782. doi: 10.3906/kim-1312-28

36. Rahimi R, Tadjarodi A, Imani M, Rabbani M, Moghaddam SS, Kerdari H. Synthesis of tetrakis(carboxyphenyl)porphyrin coated paramagnetic iron oxide nanoparticles via amino acid for photodegradation of methylene blue. Turkish Journal of Chemistry 2013; 37 (6): 879–888. doi: 10.3906/kim-1204-19

37. Ahankar H, Ramazani A, Slepokura K, Lis T, Joo SW. One-pot synthesis of substituted 4H-chromenes by nickel ferrite nanoparticles as an efficient and magnetically reusable catalyst. Turkish Journal of Chemistry 2018; 42 (3): 719–734. doi:10.3906/kim-1710-14

38. Hassani A, Eghbali P, Ekicibil A, Metin Ö. Monodisperse cobalt ferrite nanoparticles assembled on mesoporous graphitic carbon nitride (CoFe2O4/mpg-C3N4): A magnetically recoverable nanocomposite for the photocatalytic degradation of organic dyes. Journal of Magnetism and Magnetic Materials 2018; 456: 400–412. doi: 10.1016/j.jmmm.2018.02.067

39. Hassani A, Çelikdağ G, Eghbali P, Sevim M, Karaca S et al. Heterogeneous sono-Fenton-like process using magnetic cobalt ferrite-reduced graphene oxide (CoFe2O4-rGO) nanocomposite for the removal of organic dyes from aqueous solution. Ultrasonics Sonochemistry 2018; 40: 841–852. doi: 10.1016/j.ultsonch.2017.08.026

40. Xie Y, Yan B, Xu H, Chen J, Liu Q et al. Highly regenerable mussel-inspired Fe3O 4@Polydopamine-Ag core-shell microspheres as catalyst and adsorbent for methylene blue removal. ACS Appl Mater Interfaces 2014; 6: 8845–8852. doi: 10.1021/am501632f

41. Elmacı G. Magnetic Hollow Biocomposites Prepared from Lycopodium clavatum Pollens as Efficient Recyclable Catalyst. ChemistrySelect 2020; 5 (7): 2225–2231. doi: 10.1002/slct.201904152

42. Elmacı G, Frey CE, Kurz P, Zümreoğlu-Karan B. Water oxidation catalysis by birnessite@iron oxide core-shell nanocomposites. Inorganic Chemistry 2015; 54 (6): 2734-2741. doi: 10.1021/ic502908w

43. Elmacı G. Microwave-assisted rapid synthesis of C@Fe3O4 composite for removal of microplastics from drinking water. Adıyaman University Journal of Science 2020; 10 (1): 207-217. doi: 10.37094/adyujsci.739599

44. Fan R, Min H, Hong X, Yi Q, Liu W, Zhang Q et al. Plant tannin immobilized Fe3O4@SiO2 microspheres: A novel and green magnetic bio-sorbent with superior adsorption capacities for gold and palladium. Journal of Hazardous Materials 2019; 364: 780–790. doi: 10.1016/j.jhazmat.2018.05.061

45. Dippong T, Levei EA, Goga F, Cadar O. Influence of Mn2+ substitution with Co2+ on structural, morphological and coloristic properties of MnFe2O4/SiO2 nanocomposites. Materials Characterization 2021; 172: 110835. doi: 10.1016/j.matchar.2020.110835

46. Dippong T, Levei EA, Lengauer CL, Daniel A, Toloman D et al. Investigation of thermal, structural, morphological and photocatalytic properties of CuxCo1-xFe2O4 (0 ≤ x ≤ 1) nanoparticles embedded in SiO2 matrix. Materials Characterization 2020; 163: 110268. doi: 10.1016/j.matchar.2020.110268

47. Nadaf NY, Kanase SS. Biosynthesis of gold nanoparticles by Bacillus marisflavi and its potential in catalytic dye degradation. Arabian Journal of Chemistry 2019; 12 (8): 4806–4814. doi: 10.1016/j.arabjc.2016.09.020

48. Jyoti K, Singh A. Green synthesis of nanostructured silver particles and their catalytic application in dye degradation. Journal of Genetic Engineering and Biotechnology 2016; 14 (2): 311–317. doi: 10.1016/j.jgeb.2016.09.005

49. Veisi H, Azizi S, Mohammadi P. Green synthesis of the silver nanoparticles mediated by Thymbra spicata extract and its application as a heterogeneous and recyclable nanocatalyst for catalytic reduction of a variety of dyes in water. Journal of Cleaner Production 2018; 170: 1536–1543. doi: 10.1016/j.jclepro.2017.09.265

50. Gao P, Tian X, Yang C, Zhou Z, Li Y, Wang Y et al. Fabrication, performance and mechanism of MgO meso-/macroporous nanostructures for simultaneous removal of As(III) and F in a groundwater system. Environmental Science: Nano 2016; 3 (6): 1416–1424. doi: 10.1039/C6EN00400H

51. Kaloti M, Kumar A. Sustainable Catalytic Activity of Ag-Coated Chitosan-Capped γ-Fe 2 O 3 Superparamagnetic Binary Nanohybrids (Ag-γ-Fe2O3@CS) for the Reduction of Environmentally Hazardous Dyes-A Kinetic Study of the Operating Mechanism Analyzing Methyl Orange Reductio. ACS Omega 2018; 3 (2): 1529–1545. doi: 10.1021/acsomega.7b01498

52. Cheng XQ, Wang ZX, Guo J, Ma J, Shao L. Designing Multifunctional Coatings for Cost-Effectively Sustainable Water Remediation. ACS Sustainable Chemistry & Engineering 2018; 6 (2): 1881–1890. doi: 10.1021/acssuschemeng.7b03296

53. Das R, Sypu VS, Paumo HK, Bhaumik M, Maharaj V, Maity A. Silver decorated magnetic nanocomposite (Fe3O4@PPy-MAA/Ag) as highly active catalyst towards reduction of 4-nitrophenol and toxic organic dyes. Applied Catalysis B: Environmental 2019; 244: 546–558. doi: 10.1016/j.apcatb.2018.11.073

54. Abay AK, Chen X, Kuo D-H. Highly efficient noble metal free copper nickel oxysulfide nanoparticles for catalytic reduction of 4-nitrophenol, methyl blue, and rhodamine-B organic pollutants. New Journal Chemistry 2017; 41 (13): 5628–5638. doi: 10.1039/C7NJ00676D

55. Xu Y, Shi X, Hua R, Zhang R, Yao Y et al. Remarkably catalytic activity in reduction of 4-nitrophenol and methylene blue by Fe3O4@COF supported noble metal nanoparticles. Applied Catalysis B: Environmental 2020; 260: 118142. doi: 10.1016/j.apcatb.2019.118142

56. Xu P, Cen C, Zheng M, Wang Y, Wu Z et al. A facile electrostatic droplets assisted synthesis of copper nanoparticles embedded magnetic carbon microspheres for highly effective catalytic reduction of 4-nitrophenol and Rhodamine B. Materials Chemistry and Physics 2020; 253: 123444. doi: 10.1016/j.matchemphys.2020.123444

57. Cui K, Yan B, Xie Y, Qian H, Wang X et al. Regenerable urchin-like Fe3O4 @PDA-Ag hollow microspheres as catalyst and adsorbent for enhanced removal of organic dyes. Journal of Hazardous Materials 2018; 350: 66–75. doi: 10.1016/j.jhazmat.2018.02.011

58 Yang Y, Ji H, Duan H, Fu Y, Xia S et al. Controllable synthesis of mussel-inspired catechol-formaldehyde resin microspheres and their silver-based nanohybrids for catalytic and antibacterial applications. Polymer Chemistry 2019; 10 (33): 4537–4550. doi: 10.1039/C9PY00846B

59. Sun L, He J, An S, Zhang J, Zheng J et al. Recyclable Fe3O4@SiO2-Ag magnetic nanospheres for the rapid decolorizing of dye pollutants. Chinese Journal of Catalysis 2013; 34 (7): 1378–1385. doi: 10.1016/s1872-2067(12)60605-6

60. Veisi H, Razeghi S, Mohammadi P, Hemmati S. Silver nanoparticles decorated on thiol-modified magnetite nanoparticles (Fe3O4/SiO2 -Pr-S-Ag) as a recyclable nanocatalyst for degradation of organic dyes. Materials Science and Engineering: C 2019; 97: 624–631. doi: 10.1016/j.msec.2018.12.076

61. Wang Y, Gao P, Wei Y, Jin Y, Sun S et al. Silver nanoparticles decorated magnetic polymer composites (Fe3O4@PS@Ag) as highly efficient reusable catalyst for the degradation of 4-nitrophenol and organic dyes. Journal of Environmental Management 2021; 278: 111473. doi: 10.1016/j.jenvman.2020.111473

62. Gürbüz MU, Ertürk AS. Synthesis and Characterization of Jeffamine Core PAMAM Dendrimer-Silver Nanocomposites (Ag JCPDNCs) and Their Evaluation in The Reduction of 4-Nitrophenol. Journal of the Turkish Chemical Society Section A: Chemistry 2018: 5 (2): 885–894. doi: 10.18596/jotcsa.428572

63. Corma A, Concepción P, Serna P. A Different Reaction Pathway for the Reduction of Aromatic Nitro Compounds on Gold Catalysts. Angewandte Chemie 2007; 46 (41): 7820-7822. doi: 10.1002/ange.200700823

64. Zhang J, Fang Q, Duan J, Xu H, Xu H et al. Magnetically Separable Nanocatalyst with the Fe3O4 Core and Polydopamine-Sandwiched Au Nanocrystal Shell. Langmuir 2018; 34 (14): 4298–306. doi: 10.1021/acs.langmuir.8b00302

65. Qin L, Huang D, Xu P, Zeng G, Lai C et al. In-situ deposition of gold nanoparticles onto polydopamine-decorated g-C3N4 for highly efficient reduction of nitroaromatics in environmental water purification. Journal of Colloid and Interface Science 2019; 534: 357–369. doi: 10.1016/j.jcis.2018.09.051

66. Ajitha B, Reddy YAK, Lee Y, Kim MJ, Ahn CW. Biomimetic synthesis of silver nanoparticles using Syzygium aromaticum (clove) extract: Catalytic and antimicrobial effects. Applied Organometallic Chemistry 2019; 33 (5): e4867. doi: 10.1002/aoc.4867

67. Sharma G, Jeevanandam P. A facile synthesis of multifunctional iron oxide@Ag core-shell nanoparticles and their catalytic applications. European Journal of Inorganic Chemistry 2013: 6126–6136. doi: 10.1002/ejic.201301193

68. Upoma BP, Mahnaz F, Rahman Sajal W, Zahan N, Hossain Firoz MS et al. Bio-inspired immobilization of silver and gold on magnetic graphene oxide for rapid catalysis and recyclability. Journal of Environmental Chemical Engineering 2020; 8 (3): 103739. doi: 10.1016/j.jece.2020.103739

69. Liao G, Li Q, Zhao W, Pang Q, Gao H et al. In-situ construction of novel silver nanoparticle decorated polymeric spheres as highly active and stable catalysts for reduction of methylene blue dye. Applied Catalysis A: General 2018; 549: 102–111. doi: 10.1016/j.apcata.2017.09.034

70. Amir M, Güner S, Yıldız A, Baykal A. Magneto-optical and catalytic properties of Fe3O4@HA@Ag magnetic nanocomposite. Journal of Magnetism and Magnetic Materials 2017; 421: 462–471. doi: 10.1016/j.jmmm.2016.08.037

71. Amir M, Kurtan U, Baykal A. Rapid color degradation of organic dyes by Fe3O4@His@Ag recyclable magnetic nanocatalyst. Journal of Industrial and Engineering Chemistry 2015; 27: 347–353. doi: 10.1016/j.jiec.2015.01.013

72. Ismail M, Khan MI, Khan SB, Akhtar K, Khan MA et al. Catalytic reduction of picric acid, nitrophenols and organic azo dyes via green synthesized plant supported Ag nanoparticles. Journal of Molecular Liquids 2018; 268: 87-101. doi: 10.1016/j.molliq.2018.07.030

73. Sharif HMA, Mahmood A, Cheng H-Y, Djellabi R, Ali J et al. Fe3O4 Nanoparticles Coated with EDTA and Ag Nanoparticles for the Catalytic Reduction of Organic Dyes from Wastewater. ACS Applied Nano Materials 2019; 2 (8): 5310–5319. doi: 10.1021/acsanm.9b01250

74. Kurtan U, Amir M, Baykal A. Fe3O4@Nico-Ag magnetically recyclable nanocatalyst for azo dyes reduction. Applied Surface Science 2016; 363: 66–73. doi: 10.1016/j.apsusc.2015.11.214

75. Zhang M, Li M, Yu N, Su S, Zhang X. Fabrication of AgCl@tannic acid-cellulose hydrogels for NaBH4-mediated reduction of 4-nitrophenol. Cellulose 2021; 28 (6): 3515–3529. doi: 10.1007/s10570-021-03721-0